Increased tropical Atlantic wind shear in model projections of global warming

Gabriel A. Vecchi[1] and Brian J. Soden[2]

[1]   To help understand possible impacts of anthropogenic greenhouse warming on hurricane activity, we assess model-projected changes in large-scale environmental factors tied to variations in hurricane statistics. This study focuses on vertical wind shear (V_s) over the tropical Atlantic during hurricane season, the increase of which has been historically associated with diminished hurricane activity and intensity. A suite of state-of-the-art global climate model experiments is used to project changes in V_s over the 21st century. Substantial increases in tropical Atlantic and East Pacific shear are robust features of these experiments, and are shown to be connected to the model-projected decrease in the Pacific Walker circulation. The relative changes in shear are found to be comparable to those of other large-scale environmental parameters associated with Atlantic hurricane activity. The influence of these V_s changes should be incorporated into projections of long-term hurricane activity.   **Citation:**   Vecchi, G. A., and B. J. Soden (2007), Increased tropical Atlantic wind shear in model projections of global warming, *Geophys. Res. Lett.*, *34*, L08702, doi:10.1029/2006GL028905.

1.   Introduction

[2]   Empirical relationships and dynamical considerations have identified several environmental factors that influence the development of tropical cyclones. Understanding the response of these environmental parameters to a warming climate, and the consequent changes in tropical cyclones, is a topic of profound societal significance and of intense scientific debate [e.g., *Goldenberg et al.*, 2001; *Knutson and Tuleya*, 2004; *Emanuel*, 2005; *Pielke et al.*, 2005; *Webster et al.*, 2005; *Zhang and Delworth*, 2006]. Variations in tropical cyclone characteristics have been connected to thermodynamic conditions, as well as changes in atmospheric circulation [e.g., *Gray*, 1984; *Emanuel*, 1995, 2005; *Holland*, 1997; *Knutson and Tuleya*, 2004; *Webster et al.*, 2005; *Camargo et al.*, 2007; *Knutson et al.*, 2007].

[3]   Of particular importance is the vertical wind shear (V_s) which acts to inhibit tropical cyclone development [e.g., *Pielke and Landsea*, 1999; *Goldenberg et al.*, 2001; *Emanuel and Nolan*, 2004; *Camargo et al.*, 2007] and has a deleterious effect on the intensity of developed tropical cyclones [e.g., *DeMaria*, 1996; *Frank and Ritchie*, 2001]. The impact can be substantial for $V_s > 10$ ms^{-1}, with one modeling study finding that "[s]trong shear of 15 ms^{-1} literally tore an intense storm apart in about one day" [*Frank and Ritchie*, 2001].

2.   Model-Projected Changes in Vertical Wind Shear

[4]   We explore 21st Century projected changes in V_s over the tropical Atlantic and its ties to the Pacific Walker circulation, using a suite of coupled ocean-atmosphere models forced by emissions Scenario A1B (atmospheric CO_2 stabilization at 720 ppm by year 2100) for the Intergovernmental Panel on Climate Change 4th Assessment Report (IPCC-AR4). Changes are computed between two 20-year periods: 2001–2020 and 2081–2100 (use of linear trends or other averaging periods does not alter the character of the results presented here). Our index of the strength of the Pacific Walker circulation is the difference of SLP averaged over the eastern (160°W–80°W, 5°S–5°N) and western (80°E–160°E, 5°S–5°N) equatorial Pacific Ocean [*Vecchi et al.*, 2006; *Vecchi and Soden*, 2007, hereinafter referred to as VS07]. We define V_s as the magnitude of the vector difference between monthly-mean winds at 850 hPa and 200 hPa ($V_s = |\boldsymbol{u}_{850} - \boldsymbol{u}_{200}|$) following a typical V_s definition in the literature [e.g., *Goldenberg et al.*, 2001; *Zhang and Delworth*, 2006]. For models where daily data was available we found little difference in the 21st Century V_s changes computed using daily winds and monthly winds over the global tropics. See Auxiliary Material Text S1 for a list of models used.[1] We restrict our attention to changes in V_s during the northern Atlantic hurricane season (Jun.–Nov.), though the results hold for other subsets of boreal summer/fall months.

[5]   Figure 1a shows the 18-model ensemble-mean projected change in V_s (normalized per °C global warming) over the 21st Century; for reference, contours show the background V_s. There is a prominent increase in V_s over the tropical Atlantic and East Pacific (10°N–25°N) (Figure 1a), which is distinct from a tendency for weakened V_s across much of the northern hemisphere tropics (see below). The amplitude of the projected V_s increase is considerable, given the 1.5–3.5°C global-mean surface air temperature increase in these models by the end of the 21st Century [*Held and Soden*, 2006; VS07]. These V_s changes are robust across the multi-model suite, with all but a handful of models projecting an increase in the 21st Century (Figure 1b). We define the tropical Atlantic region in which there is large increase of V_s in the ensemble mean (90°W–40°W, 13°N–25°N) as the "Shear Enhancement Region" or SER (see

[1]Geophysical Fluid Dynamics Laboratory, National Oceanic and Atmospheric Administration, Princeton, New Jersey, USA.
[2]School for Marine and Atmospheric Science, University of Miami, Miami, Florida, USA.
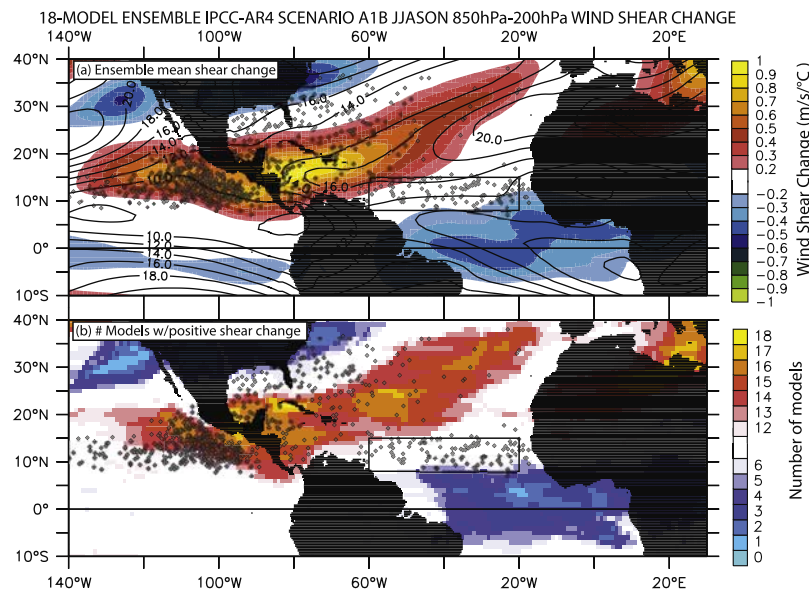
18-MODEL ENSEMBLE IPCC-AR4 SCENARIO A1B JJASON 850hPa-200hPa WIND SHEAR CHANGE

Figure 1. IPCC-AR4 multi-model projections of June–November V_s change. (a) The 18-model ensemble-mean change in June–November 850 hPa-200 hPa vertical wind shear (shaded, ms^{-1} °C^{-1} warming), contours show ensemble-mean background shear (2001–2020 average, ms^{-1}); (b) Number of models (out of 18) showing positive change in V_s. Changes are normalized by each model's global mean June–November surface air temperature change before averaging. Dots indicate locations of tropical cyclone genesis over the period 1981–2005; box indicates a region of frequent cyclone development (MDR).

Figure 2a). The Scenario A1B 21st Century V_s changes in the SER are between -2% and 30% of the mean shear.

[6] On interannual timescales, changes in the Pacific Walker circulation associated with El Niño have been connected to enhanced shear over the tropical Atlantic, via atmospheric teleconnections from the related eastward shift of equatorial Pacific atmospheric convection [e.g., *Pielke and Landsea*, 1999; *Camargo et al.*, 2007]. Here we explore the extent to which the model-projected increase in V_s is related to the model projections of a weakened Pacific Walker circulation over the 21st Century [e.g., *Held and Soden*, 2006; VS07]. Figure 2a shows the inter-model correlation between the change in the Pacific Walker circulation index and the change in V_s at each location; warm colors in Figure 2a indicate regions where a decrease

in the Pacific Walker circulation is associated with increased shear. Notice that the region of strongest correlation corresponds to the SER. That is, inter-model differences in the region of largest ensemble-mean shear increase are correlated to the deceleration of the Walker circulation in each model. The connection between decreased Pacific Walker circulation and increased shear in these models is further highlighted in Figure 2b. The models with larger Walker circulation weakening tend to show larger V_s increase over the SER region (the correlation coefficient across models is 0.71; $p < 0.05$).

[7] We note that the SER is displaced to the north of the region of most frequent cyclogenesis over the period 1981–2005, which we shall refer to as the "Main Development Region" or MDR (60°W–20°W, 8°N–15°N; see Figure 1).
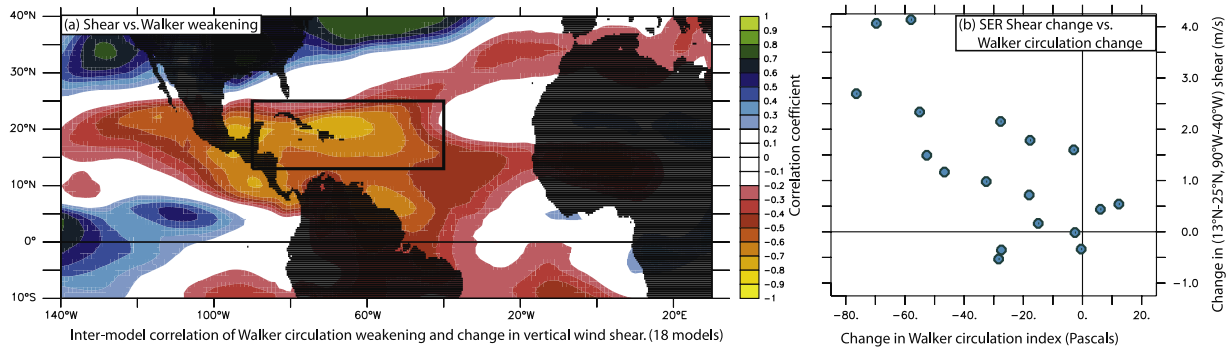

Figure 2. Relationship between IPCC-AR4 multi-model projections of June–November 850 hPa-200 hPa V_s change and Pacific Walker circulation change. (a) The 18-model inter-model correlation of V_s change at each point and Pacific Walker circulation change; (b) Change in the SER (90°W–40°W, 13°N–25°N) V_s change versus Pacific Walker circulation change in each model. Pacific Walker circulation index defined as sea level pressure difference between eastern and western equatorial Pacific [*Vecchi et al.*, 2006; *Vecchi and Soden*, 2007]. Box in Figure 2a indicates the region of strong ensemble mean shear increase (SER).
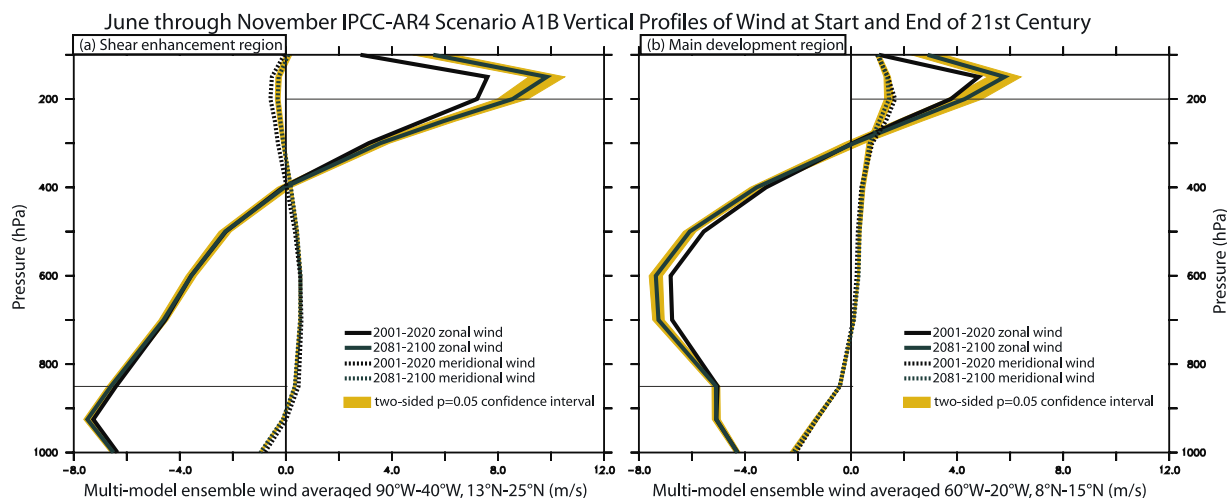
Figure 3. Profiles of June–November winds at start (black lines) and end (green lines) of 21st century from IPCC-AR4 Scenario A1B multi-model ensemble averaged over two regions in north tropical Atlantic. Zonal (meridional) winds are shown in solid (dotted) lines; orange shading shows the two-sided $p = 0.05$ interval on the 2081–2100 average based on a *Student's-t* test and the inter-model variance. (left) Region of robust V_s increase indicated in Figure 2a. (right) Region of frequent tropical cyclone formation indicated in Figure 1. Light horizontal lines indicate 850 hPa and 200 hPa.

We chose to define V_s as $|\mathbf{u}_{850} - \mathbf{u}_{200}|$ because there is substantial literature indicating some relationship between V_s defined in this manner and hurricanes. Over the SER this definition captures the principal wind features that contribute to vertical shear (Figure 3a). However, over the MDR, both the model background and ensemble-mean change of tropospheric vertical wind shear are better captured by the difference between 700 hPa and 150 hPa winds (Figure 3b). The IPCC-AR4 models show a statistically significant ($p <$ 0.05) increase in MDR shear between 700 hPa and 150 hPa (Figure 3b). To the extent that the effect of an increase of 700 hPa to 150 hPa wind shear of equal relevance to that of 850 hPa to 200 hPa wind shear, the multi-model ensemble also projects an increase in shear over the MDR. If one adopts an alternative definition for vertical shear as the vertical standard deviation of wind over the model free troposphere (850 hPa–150 hPa), rather than the magnitude of the vector difference at two pressure levels, the models project a substantial increase of shear over both the MDR and SER (not shown).

[8] So far we have focused on the June–November tropical North Atlantic shear, though there are robust V_s changes evident globally, in other seasons (e.g., auxiliary material) and in the annual mean. For example, between $20°–40°$ latitude in the southern hemisphere (and both hemispheres in the annual-mean) there is a zonally-symmetric V_s increase (e.g., Figure 4a). Within $5°$ of the Equator there is a noticeable weakening of V_s over all three oceanic basins (Figure 4a), which is present in all seasons. In these models the near-equatorial V_s weakening appears related to their robust weakening of near-equatorial zonal overturning [e.g., *Vecchi et al.*, 2006; VS07], resulting from global thermodynamic constraints [*Held and Soden*, 2006].

3.   Changes in Other Hurricane-Related Indices

[9] Increases in lower tropospheric absolute vorticity (η_{850}), mid-tropospheric relative humidity (rh_{700}) and

Emanuel's [1995] hurricane maximum potential intensity for velocity (MPI_v) have been linked to increased hurricane activity. *Emanuel and Nolan* [2004] have developed a "Cyclone Genesis Potential Index" – or GPI – which looks at the combined effect of all four parameters on storm genesis. As is shown in the auxiliary material, changes in the various terms would have comparable effects on *GPI* if their fractional changes are similar. In Figure 4 we compare the fractional changes in the parameters relevant to *GPI*.

[10] The changes in η_{850} are an order of magnitude smaller than those of the other parameters and therefore not shown. The tropical Atlantic rh_{700} changes are dominated by drying over the Caribbean Sea (Figure 4b). Tropical-mean rh_{700} shows very little change, consistent with the largely Clausius-Clapeyron driven increase in specific humidity of these models [*Held and Soden*, 2006]. Many of the regional rh_{700} changes appear connected to the local changes in 500 hPa pressure velocity (ω_{500}, contours in Figure 4b), with regions of anomalous descent (ascent) showing relative drying (moistening)-a relationship consistent with anomalous advection of drier (moister) air from above (below).

[11] While June–November MPI_v increases over most of the northern hemisphere tropics, there is a large region in the northern tropical Atlantic where the ensemble-mean MPI_v actually decreases (Figure 4c). This region of MPI_v decrease is associated with a relative minimum in the sea surface temperature (SST) warming (contours in Figure 4c). MPI_v changes around the globe track the structure of SST changes very tightly – with regions that warm more (less) than the tropical mean showing an MPI increase (decrease). Since changes in upper tropospheric temperatures are determined by changes in the tropical-mean SST, rather than changes in local SST [e.g., *Sobel et al.*, 2002], a local minimum (maximum) in surface warming results in an anomalous increase (decrease) in static stability. This relationship between MPI_v and local SST changes (relative to the tropical mean SST change) holds not only for the ensemble mean, but also for each of the models. A similar
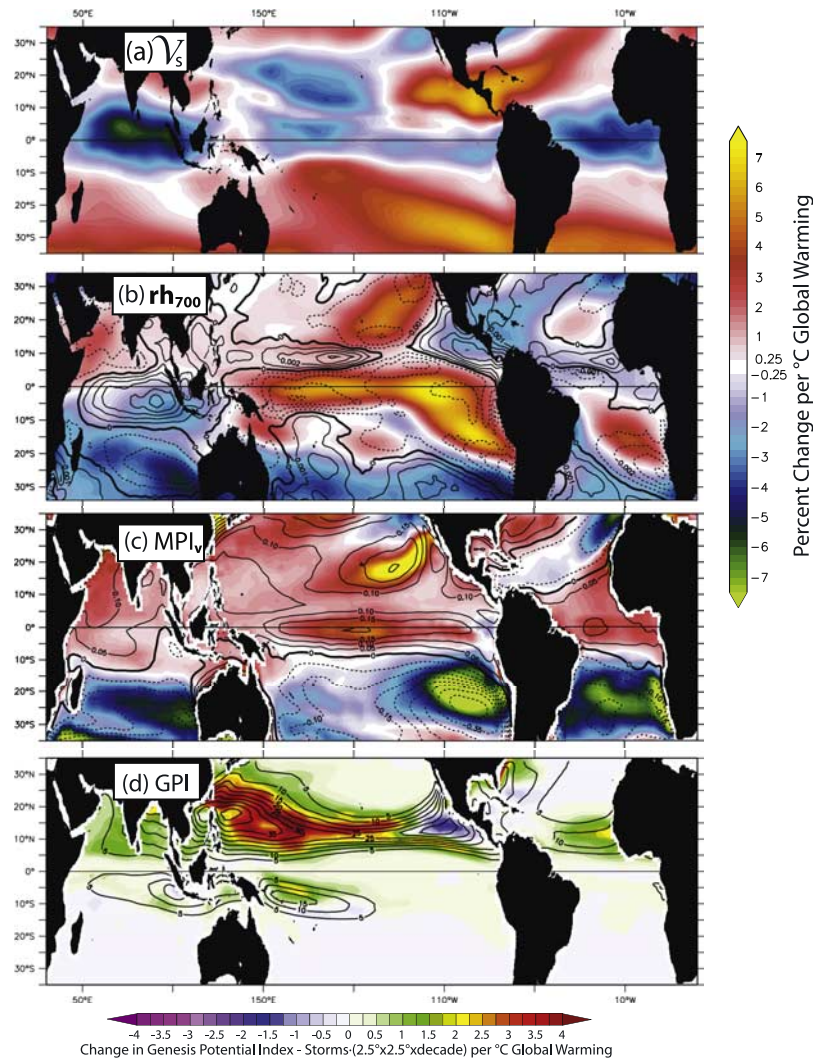
Figure 4. IPCC-AR4 Scenario A1B June–November ensemble mean projected fractional change in large-scale environmental parameters associated with hurricane intensity and activity: (a) V_s, (b) 700 hPa relative humidity, and (c) *Emanuel*'s [1995] wind maximum potential intensity (MPI_v). (d) Change in *Emanuel and Nolan*'s [2004] genesis potential index (GPI) is shown. Fractional changes are normalized by global surface air temperature increase. Contoured in Figure 4b is the ensemble-mean 500 hPa pressure velocity (ω_{500}) change (normalized by each model's global mean surface temperature change), upward motion is negative. Contoured in Figure 4c is the difference between the local SST change and the $35°S–35°N$ mean SST change, normalized by the $35°S–35°N$ mean SST change. Contoured in Figure 4d is the ensemble-mean GPI averaged over the period 2001–2020.

mechanism has been suggested to be important in the El Niño response of tropical Atlantic hurricane activity [*Tang and Neelin*, 2004]. Understanding the processes that control both regional and global tropical SST changes [e.g., *Knutson et al.*, 2006; *Santer et al.*, 2006] is essential for projecting regional MPI_v changes. The SST warming minimum in the tropical Atlantic is also present in the ensemble-mean of IPCC-AR4 climate model runs with a mixed-layer ocean forced with a doubling of CO_2 (not shown), suggesting that the minimum in surface warming may result primarily from changes in atmospheric forcing, rather than from ocean dynamics.

[12] The multi-model ensemble-mean change in *GPI* is shown in Figure 4d. Model-projected *GPI* increases substantially in the western and central Pacific, but the changes in the tropical Atlantic and East Pacific are more

modest – showing both regions of increase and decrease – due in part to the local increase in wind shear (e.g., Auxiliary Figure S1). In the multi-model ensemble, the North Atlantic and East Pacific contribution of V_s to the fractional change in GPI is comparable to that of each of the other three terms (Auxiliary Figure S1), although the region of largest percentage Atlantic GPI changes caused by shear is a region of relatively modest GPI.

4. Summary and Discussion

[13] Global climate model projections for the 21st Century indicate a robust increase in June–November vertical wind shear in the tropical Atlantic and East Pacific Oceans. Over the Caribbean Sea, the northern tropical Atlantic (the SER) and the eastern tropical Pacific, the multi-model

ensemble-mean shear increases by 0.5-1 ms^{-1} per °C global warming (Figures 1 and 3). The Atlantic shear changes result largely from changes to upper tropospheric zonal winds (Figure 3). Aspects of the projected shear increase in the SER are strongly related to a reduction in Pacific Walker circulation, with the inter-model variability in Walker circulation changes explaining ~50% of the inter-model variability in SER shear change (Figure 2). The relative amplitude of the shear increase in these models is comparable to or larger than model-projected changes in other large-scale parameters related to tropical cyclone activity (Figure 4), indicating that these shear changes should be considered in projections of future changes in tropical cyclone activity. Based on published connections between large-scale environmental parameters and hurricane activity [e.g., *Emanuel and Nolan*, 2004], the changes shown here alone would not suggest a strong anthropogenic increase in tropical Atlantic or East Pacific hurricane activity during the 21st Century; although other regions (e.g., Indian and western/central Pacific oceans) show consistent changes towards more hurricane-favorable conditions (Figure 4).

[14] In addition to impacting cyclogenesis, the increase in SER shear could act to inhibit the intensification of tropical cyclones as they traverse from the MDR to the Caribbean and North America (e.g., Auxiliary Material Figure S2). Although the response of the frequency and intensity of tropical storms to the shear changes documented here remains to be fully understood, the robustness of the shear changes across models, their impact on GPI (Figure 4d and Auxiliary Material Figure S1), and the potential influence of shear on cyclone intensity underscore their importance in projections of future Atlantic hurricane activity.

[15] The detailed mechanisms behind the modeled Tropical Atlantic V_s changes should be comprehensively explored, in order to fully understand the robustness and limitations of the model V_s projections. For example, the extent to which El Niño serves as a useful analogue for the mechanisms behind the projected shear changes should be further examined: although the sign of the relationship in Figure 2 is the same as during El Niño, the structure of the V_s changes differs from that associated with El Niño. It is also important to keep in mind that the Pacific Walker circulation can exhibit energetic variability – even on decadal timescales – independently of external forcing [e.g., *Vecchi et al.*, 2006], and that Atlantic shear is influenced by a variety of factors besides the Pacific Walker circulation. For example, both the meridional temperature gradient in the tropical Atlantic [e.g., *Zhang and Delworth*, 2006] and the extent of the Atlantic Warm Pool [e.g., *Wang et al.*, 2006] have been connected to changes in V_s. A full understanding of the projected and historical patterns of tropical Atlantic shears must take into consideration the full set of factors that influence shear, including those resulting from internal climate variability as well as forced climate change.

References

Camargo, S. J., K. A. Emanuel, and A. H. Sobel (2007), Use of genesis potential index to diagnose ENSO effects upon tropical cyclone genesis, *J. Clim.*, in press.

DeMaria, M. (1996), The effect of vertical shear on tropical cyclone intensity change, *J. Atmos. Sci.*, *53*(14), 2076–2087.

Emanuel, K. A. (1995), Sensitivity of tropical cyclones to surface exchange coefficients and a revised steady-state model incorporating eye dynamics, *J. Atmos. Sci.*, *52*, 3969–3976.

Emanuel, K. A. (2005), Increasing destructiveness of tropical cyclones over the past 30 years, *Nature*, *436*, 686–688.

Emanuel, K. A., and D. S. Nolan (2004), Tropical cyclones and the global climate system, paper presented at 26th Conference on Hurricanes and Tropical Meteorology, Am. Meteorol. Soc., Miami, Fla.

Frank, W. M., and E. A. Ritchie (2001), Effects of vertical wind shear on the intensity and structure of numerically simulated hurricanes, *Mon. Weather Rev.*, *129*, 2249–2269.

Goldenberg, S. B., C. Landsea, A. M. Mestas-Nunez, and W. M. Gray (2001), The recent increase in Atlantic hurricane activity, *Science*, *293*, 474–479.

Gray, W. M. (1984), Atlantic seasonal hurricane frequency. Part I: El Niño and 30 mb quasi-biennial oscillation influences, *Mon. Weather Rev.*, *112*, 1649–1668.

Held, I. M., and B. J. Soden (2006), Robust responses of the hydrological cycle to global warming, *J. Clim.*, *19*, 5686–5699.

Holland, G. J. (1997), The maximum potential intensity of tropical cyclones, *J. Atmos. Sci.*, *54*, 2519–2541.

Knutson, T. R., and R. E. Tuleya (2004), Impact of CO_2-induced warming on simulated hurricane intensity and precipitation: Sensitivity to the choice of climate model and convective parameterization, *J. Clim.*, *17*, 3477–3495.

Knutson, T. R., et al. (2006), Assessment of Twentieth-Century regional surface temperature trends using the GFDL CM2 coupled models, *J. Clim.*, *19*, 1624–1651.

Knutson, T. R., J. J. Sirutis, S. T. Garner, I. M. Held, and R. E. Tuleya (2007), Simulation of the recent multi-decadal increase of Atlantic hurricane activity using an 18-km grid regional model, *Bull. Am. Meteorol. Soc.*, in press.

Pielke, R. A., and C. W. Landsea (1999), La Niña, El Niño, and Atlantic hurricane damages in the United States, *Bull. Am. Meteorol. Soc.*, *80*, 2027–2033.

Pielke, R. A., C. Landsea, M. Mayfield, J. Laver, and R. Pasch (2005), Hurricanes and global warming, *Bull. Am. Meteorol. Soc.*, *86*, 1571–1575.

Santer, B. D., et al. (2006), Forced and unforced ocean temperature changes in Atlantic and Pacific tropical cyclogenesis regions, *Proc. Natl. Acad. Sci. U. S. A.*, *103*, 13,905–13,910, doi:10.1073/pnas.0602861103.

Sobel, A. H., I. M. Held, and C. S. Bretherton (2002), The ENSO signal in tropical tropospheric temperature, *J. Clim.*, *15*, 2702–2706.

Tang, B. H., and J. D. Neelin (2004), ENSO Influence on Atlantic hurricanes via tropospheric warming, *Geophys. Res. Lett.*, *31*, L24204, doi:10.1029/2004GL021072.

Vecchi, G. A., and B. J. Soden (2007), Global warming and the weakening of the tropical circulation, *J. Clim.*, in press.

Vecchi, G. A., B. J. Soden, A. T. Wittenberg, I. M. Held, A. Leetmaa, and M. J. Harrison (2006), Weakening of tropical Pacific atmospheric circulation due to anthropogenic forcing, *Nature*, *441*, 73–76.

Wang, C., D. B. Enfield, S.-K. Lee, and C. W. Landsea (2006), Influences of the Atlantic warm pool on western hemisphere summer rainfall and Atlantic hurricanes, *J. Clim.*, *19*, 3011–3028.

Webster, P. J., G. J. Holland, J. A. Curry, and H.-R. Chang (2005), Changes in tropical cyclone number, duration and intensity in a warming environment, *Science*, *309*, 1844–1846.

Zhang, R., and T. L. Delworth (2006), Impact of Atlantic multidecadal oscillations on India/Sahel rainfall and Atlantic hurricanes, *Geophys. Res. Lett.*, *33*, L17712, doi:10.1029/2006GL026267.

————————————

B. J. Soden, Rosenstiel School for Marine and Atmospheric Science, University of Miami, 4600 Rickenbacker Causeway, Miami, FL 33149, USA.

G. A. Vecchi, Geophysical Fluid Dynamics Laboratory, NOAA, Princeton Forrestal Campus Route 1, P.O. Box 308, Princeton, NJ 08542, USA. (gabriel.a.vecchi@noaa.gov)

Auxiliary Material to:

Increased Tropical Atlantic Wind Shear in Model Projections of Global Warming

In Geophysical Research Letters

Gabriel A. Vecchi

Geophysical Fluid Dynamics Laboratory -NOAA

Brian J. Soden

Rosenstiel School for Marine and Atmospheric Science - U. Miami

_____

Corresponding author: Dr. Gabriel A. Vecchi, Geophysical Fluid Dynamics Laboratory / NOAA, US Route 1, Forrestal Campus, Princeton, NJ 08542
Tel: (609) 452-6583, Fax: (609) 987-5063, email: gabriel.a.vecchi@noaa.gov

A-Models Used:

For our analysis we explore the 21st Century projections of the suite of coupled ocean-atmosphere models forced by emissions scenario A1B (atmospheric CO_2 stabilization at 720ppm by year 2100) for the Intergovernmental Panel on Climate Change 4th Assessment Report (IPCC-AR4). The IPCC-AR4 archive has 22 models available for the Scenario A1B, although not all fields are archived for all models *[see Table 1 Vecchi and Soden 2007, henceforthVS07, for a list of models and references]*. From this list of models, we exclude three models that have deficient Pacific Walker circulations *[VS07]*, though the principal results are not altered by their inclusion. No three dimensional data is available for one of the models in the archive (MIUB-ECHO-G), so it is not analyzed, leaving 18 models in total that we analyze.

All eighteen models had three-dimensional monthly-mean horizontal wind data available. Thus, for our analysis of vertical wind shear (V_s) we used: BCCR BCM2.0, CNRM CM3, CSIRO Mk3.0, GFDL CM2.0, GFDL CM2.1, GISS-AOM, GISS-EH, IAP FGOALS, INM CM3.0, IPSL CM4, MIROC Hi, MIROC Med, MPI ECHAM5, MRI CGCM2.3, NCAR CCSM3, NCAR PCM1, UKMet HadCM3, UKMet HadGem1; see *VS07* (Table. 1). Two models (GISS-AOM and UkMet HadCM3) did not have the data necessary for analysis of relative humidity, hurricane maximum potential intensity *[Emanuel 1995]* and genesis potential index *[Emanuel and Nolan 2004]*. So for our analysis of these quantities we only use sixteen models.

B-Contributions to Chage in Genesis Potential Index:

Based on in lower tropospheric absolute vorticity (η_{850}), mid-tropospheric relative humidity (rh_{700}) and the *Emanuel [1995]* hurricane maximum potential intensity for velocity (MPI_v), and 850hPa-200hPa vertical wind shear (V_s), *Emanuel and Nolan [2004]* have developed a "Cyclone Genesis Potential Index" – or GPI – that has been shown to correlate with the statistics of storm genesis in both observations and models *[e.g. Camargo et al. 2007a.b.]* defined as:

$$GPI = (1+0.1 \cdot V_s)^{-2} \cdot (|10^5 \eta|^{3/2}) \cdot (rh_{700}/50)^3 \cdot (MPI_v/70)^3 \qquad \text{Equation (1)}$$

From Equation (1) it can be seen that:

$$dGPI/GPI = -2\, d\xi/\xi + 1.5\, d\eta_{850}/\eta_{850} + 3drh_{700}/rh_{700} + 3dMPI_v/MPI_v \qquad \text{Equation (2)}$$

where $\xi = 1+0.1 \cdot V_s$. As shown in Fig. 4 of the main manuscript, the magnitude of the fractional changes in MPI_v, rh_{700}, and V_s are comparable. According to Equation (2) changes in the various terms would have comparable effects on *GPI* if their fractional

changes are similar. This is confirmed in Auxiliary Fig. 1, which shows that the multi-model ensemble, the contribution of V_s to the change in GPI is comparable to that of each of the other three terms.

C. Shear Impact on Storm Intensity:

In addition to the potential impact on cyclogenesis, which can be estimated using quantities such as *GPI [Emanuel and Nolan 2004]*, vertical wind shear can also adversely affect the intensification of an existing tropical cyclone *[e.g. DeMaria 1996, Frank and Ritchie 2001]*. A full understanding of the impacts of shear on tropical storm intensity should take into account possible nonlinearities in the response to shear, as well as nonlinearities in the response to both shear and other quantities (such as large-scale thermodynamic conditions). However, to the extent that the statistical relationship between storm intensification and shear described by *DeMaria [1996]* can be applied to the climate change problem, it can be used to estimate the potential impact of the ensemble-mean shear increase described above and in the main manuscript. *DeMaria [1996]* developed a regression coefficient between ambient shear (850hPa-200hPa) and the rate of change in storm intensity, which showed a latitudinal dependence. *DeMaria [1996]* computes – based on the 1989-1994 observed Atlantic hurricane database - regression coefficients of shear on intensity change, which were found to depend on storm latitude. The *DeMaria [1996]* regressions were computed using values of shear and storm intensity change normalized by the standard deviation of each quantity. To apply the regressions to storm intensification we compute the standard deviation of 12-hour storm intensification from the 1989-1994 National Hurricane Center Best Track

Data, and that of shear from the daily NCEP-NCAR Reanalysis *[Kalnay et al. 1996]* 850hPa-200hPa wind shear resampled onto the storm positions. By combining the *DeMaria [1996]* normalized regression coefficient with the shear and intensification standard deviations, the regression coefficients of shear on storm intensification are found to be become -0.23 ms^{-1} intensification per ms^{-1} shear equatorward of 29°, and -0.12 ms^{-1} intensification per ms^{-1} shear poleward of 29°.

We estimate the effect of the model-projected changes in Atlantic and East Pacific shear on storm intensity at landfall using the *DeMaria [1996]* regression, the 1965-2006 U.S. National Hurricane Center Best Track dataset for the Atlantic and East Pacific basins (since the total impact of shear on a storm will depend on its track), and the multi-model ensemble-mean projected 850hPa-200hPa wind shear changes (2081-2100 minus 2001-2020). Using the historical hurricane track data, the model-projected shear anomaly corresponding to the month of each storm position is linearly interpolated to the latitude, longitude coordinates of the storm center, and – using the *DeMaria [1996]* regression coefficient – the estimated effect of shear on storm intensification is integrated from the storm genesis to its landfall.

The linear estimate of shear impact on storm intensity at landfall is predominantly negative. The effect of the increased shear across the tropical Atlantic and East Pacific on storm intensity at landfall can be substantial (see Auxiliary Figure 2.a). Reductions in magnitude at landfall of 2-6 ms^{-1} are not uncommon, and for a handful of storms it can be larger than that. For reference Auxiliary Fig. 2.b shows the model-projected changes in

Emanuel [1995] maximum intensity of storm velocity (MPI_v) computed for the multi-model ensemble over the same period. In the tropical Atlantic, the estimates of the shear effect on storm intensity at landfall are of comparable magnitude to the model projections of MPI_v – but principally of opposite sign. Though this exploration of the possible impacts of model-projected shear on storm intensity is not definitive, it indicates that the magnitude of the impact is potentially comparable to the increase in storm potential intensity.

Thus, it appears that – in the tropical Atlantic and East Pacific Oceans - the increase in vertical wind shear could partly mitigate the increased thermodynamic tendency towards increased storm intensity. However, it is important to note that it is only in the tropical Atlantic and East Pacific Oceans that there is a projected increase of shear during the local hurricane season. In the West Pacific and Indian Oceans, the models projected a long-term decrease in vertical wind shear through the 21st Century.

D – Projected Changes in Hurricane-related Indices in Austral Summer/Fall:

Though the focus of this work has been model-projected changes during North Atlantic hurricane season (June-November), the IPCC-AR4 Scenario A1B model projections also show changes in quantities across the globe during austral winter/spring (Auxiliary Fig. 3). The shear increase in the subtropics and its increase near-Equator that was noted in June-November is also evident in the projected December-May changes. Again, tropical-mean rh_{700} shows very little change, as global-mean specific humidity changes in a manner consistent with that expected from Clausius-Clapeyron *[e.g., Held and Soden*

2006]. As noted in the main manuscript, the principal regional rh_{700} changes appear connected to the local changes in 500hPa pressure velocity (ω_{500}), with regions of anomalous descent (ascent) showing relative drying (moistening) – a relationship consistent with anomalous advection of drier (moister) air from above (below). Overall December-May MPI_v tends to increase over much of the tropics. However, there are various regions where MPI_v decreases, associated with relative minimum in the sea surface temperature (SST) warming (contours in Suppl. Fig. 3.c). The *MPIv* decrease in these regions is not likely to be of much significance to cyclogenesis, as the relative minima occur in regions of large-scale subsidence. As discussed in the main manuscript, the structure of MPI_v changes tracks that of SST change very tightly: regions that warm more (less) than the tropical mean showing an MPI increase (decrease). December-May changes in *GPI* are dominated by an increase across the southern Indian and Pacific Oceans. Except for a region of *GPI* decrease on the eastern edge of the southwest Pacific local maximum in *GPI*, the multi-model ensemble projects an overall increase in *GPI*.

References:

Camargo, S.J., A.H. Sobel, A.G. Barnston, and K.A. Emanuel, 2007.a, Tropical cyclone genesis potential index in climate models. *J. Climate (in press)*.

Camargo, S.J., K.A. Emanuel, and A.H. Sobel, 2007.b, Use of genesis potential index to diagnose ENSO effects upon tropical cyclone genesis. *J. Climate (in press)*.

DeMaria, M. (1996), The Effect of Vertical Shear on Tropical Cyclone Intensity Change. *J. Atm. Sci.*, *53*(14), 2076-2087.

Emanuel, K.A. (1995), Sensitivity of tropical cyclones to surface exchange coefficients and a revised steady-state model incorporating eye dynamics, *J. Atmos. Sci., 52*.

Frank, W.M., and E.A. Ritchie (2001), Effects of Vertical Wind Shear on the Intensity and Structure of Numerically Simulated Hurricanes, *Mon Wea Rev*, *129*, 2249-69.

Held, I. M. and B.J. Soden (2006), Robust responses of the hydrological cycle to global warming, *J. Clim., 19*.

Kalnay, E., et al. (1996), The NCEP/NCAR 40-Year Reanalysis Project, *Bull. Am. Meteorol. Soc.*, *77*, 437 – 471.

Vecchi, G.A. and B.J. Soden (2007), Global Warming and the Weakening of the Tropical Circulation, *J. Clim.*, *(in press)*.
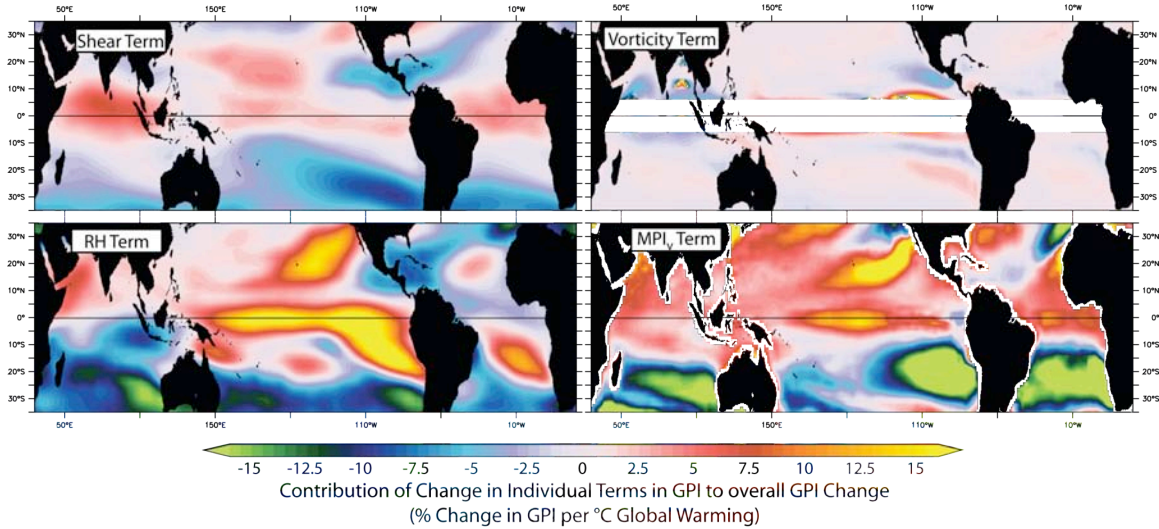
Auxiliary Figure Captions

Auxiliary Figure 1: IPCC-AR4 Scenario A1B June-November ensemble mean contribution to change in *Emanuel and Nolan [2004]* genesis potential index (GPI) of the change in the four factors that define GPI: (a) the vertical wind shear term ($-2d\xi/\xi$; where $\xi=1+0.1\,\mathcal{V}_s$), (b) the 850hPa absolute vorticity term ($3/2d|\eta_{850}|/|\eta_{850}|$), (c) 700hPa relative humidity term ($3drh_{700}/rh_{700}$), and (c) *Emanuel [1995]* wind maximum potential intensity (MPI_v) term ($3dMPI_v/MPI_v$). Fractional changes are differences between 2081-2100 and 2001-2020 average, divided by 2001-2020 average and normalized by global surface air temperature increase. Notice that the amplitude of the North Atlantic contribution to change in GPI by changes in vertical wind shear (a) is of the same order as that of the other terms (b-d). $GPI = (1+0.1\cdot\,\mathcal{V}_s\,)^{-2} \cdot (|10^5\eta|^{3/2}) \cdot (rh_{700}/50)^3 \cdot (MPI_v/70)^3$; which implies that $dGPI/GPI = -2\,d\xi/\xi + 3/2\cdot d\eta_{850}/\eta_{850} + 3drh_{700}/rh_{700} + 3dMPI_v/MPI_v$; where $\xi=1+0.1\,\mathcal{V}_s$. Thus, if the order of magnitude of the fractional changes in each of the terms is comparable, they will have impacts of a comparable order of magnitude.

Auxiliary Figure 2: Estimates of the impact of (a) shear and (b) large-scale thermodynamic conditions on North Atlantic and East Pacific tropical storms, based on the IPCC AR-4 Scenario A1B multi-model ensemble-mean change. (a) Impact of model project changes in shear to the intensity computed by applying the *DeMaria [1996]* latitude-dependent regression between shear and storm intensity change to the tropical storms in the 1965-2006 U.S. National Hurricane Center Best Track Database – sampling
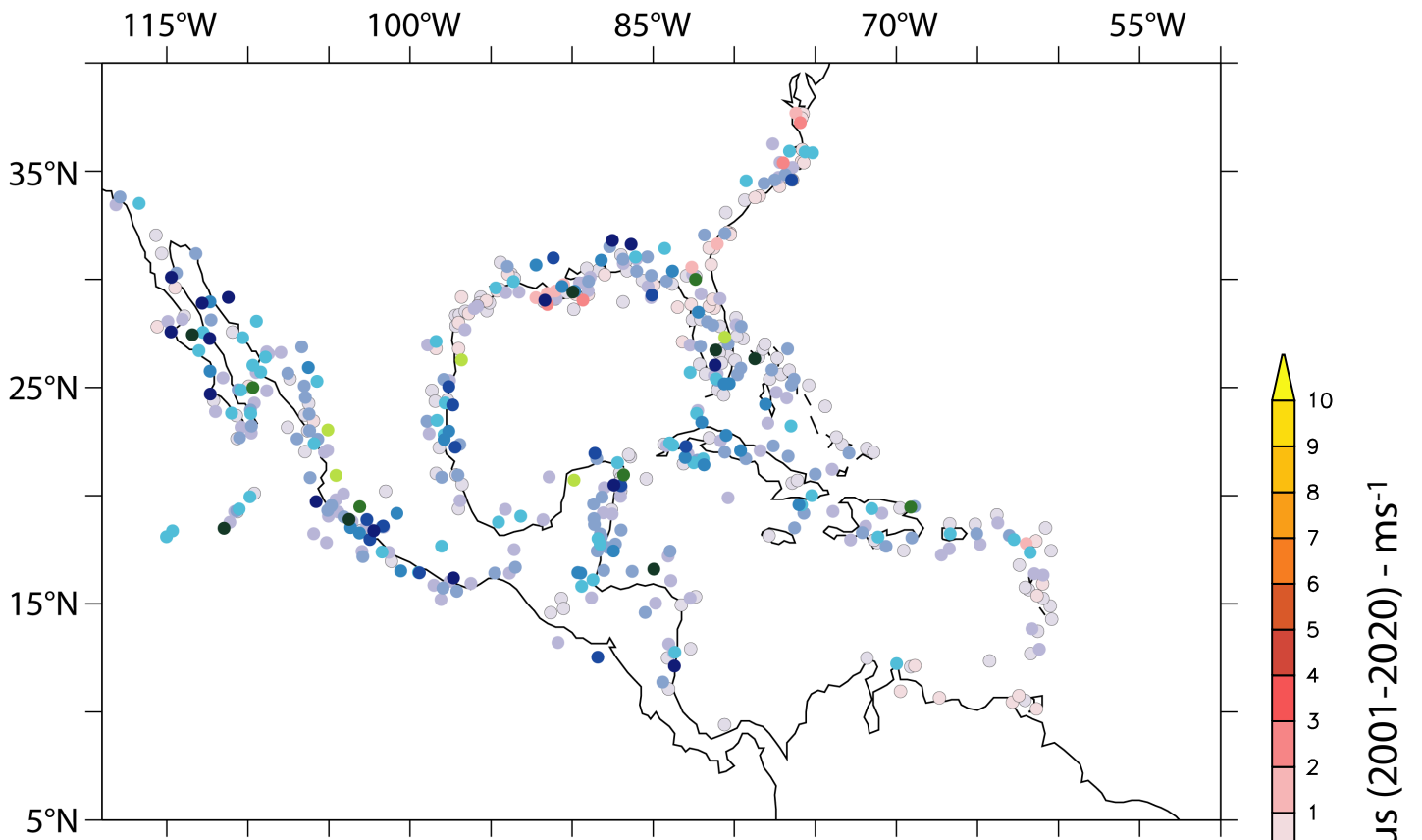
the model-projected June-November (850hPa-200hPa) shear change along the storm tracks. Symbols are plotted such that symbols of larger amplitude overlay those of lower amplitude, and when symbols have the same amplitude those of positive sign overlay those of negative sign. (b) Change in the June-November *Emanuel [1995]* maximum potential intensity of tropical storm velocity (MPI_v), for the IPCC-AR4 Scenario A1B multi-model ensemble-mean. Changes computed as differences between the period (2081-2100) and (2001-2020); units for the changes in ms^{-1}. Notice that the magnitude of the changes to intensity at storm landfall from changes in shear are comparable to those of MPI_v, and generally acting to reduce storm intensity.

Auxiliary Figure 3: Same as Figure 4 except for the six month season December-May: IPCC-AR4 Scenario A1B ensemble mean projected fractional change in large-scale environmental parameters associated with hurricane intensity and activity: (a) V_s, (b) 700hPa relative humidity, and (c) *Emanuel [1995]* wind maximum potential intensity (MPI_v). Panel (d) shows the change in *Emanuel and Nolan [2004]* genesis potential index (GPI). Fractional changes are normalized by global surface air temperature increase. Contoured in (b) is the ensemble-mean 500hPa pressure velocity (ω_{500}) change (normalized by each model's global mean surface temperature change), upward motion is negative. Contoured in (c) is the difference between the local SST change and the 35°S-35°N mean SST change, normalized by the 35°S-35°N mean SST change. Contoured in (d) is the ensemble-mean GPI averaged over the period 2001-2020.

-15   -12.5   -10   -7.5   -5   -2.5   0   2.5   5   7.5   10   12.5   15
Contribution of Change in Individual Terms in GPI to overall GPI Change
(% Change in GPI per °C Global Warming)

Supplementary Figure 1: IPCC-AR4 Scenario A1B June-November ensemble mean contribution to change in *Emanuel and Nolan [2004]* genesis potential index (GPI) of the change in the four factors that define GPI: (a) the vertical wind shear term ($-2d\xi/\xi$; where $\xi=1+0.1\,V_s$), (b) the 850hPa absolute vorticity term ($3/2d|\eta_{850}|/|\eta_{850}|$), (c) 700hPa relative humidity term ($3drh_{700}/rh_{700}$), and (c) *Emanuel [1995]* wind maximum potential intensity (MPI_v) term ($3dMPI_v/MPI_v$). Fractional changes are differences between 2081-2100 and 2001-2020 average, divided by 2001-2020 average and normalized by global surface air temperature increase. Notice that the amplitude of the North Atlantic contribution to change in GPI by changes in vertical wind shear (a) is of the same order as that of the other terms (b-d). $GPI = (1+0.1\cdot V_s)^{-2} \cdot (|10^5\eta|^{3/2}) \cdot (rh_{700}/50)^3 \cdot (MPI_v/70)^3$; which implies that $dGPI/GPI = -2\,d\xi/\xi + 3/2\cdot d\eta_{850}/\eta_{850} + 3drh_{700}/rh_{700} + 3dMPI_v/MPI_v$; where $\xi=1+0.1\,V_s$. Thus, if the order of magnitude of the fractional changes in each of the terms is comparable, they will have impacts of a comparable order of magnitude.

(a) Integrated Effect of 21st Century Shear
Change on 1965-2006 Tropical Storm Magnitude at Landfall

(b) 21st Century Change in Maximum Potential Intensity of Storm

Change (2081-2100) minus (2001-2020) - ms^{-1}
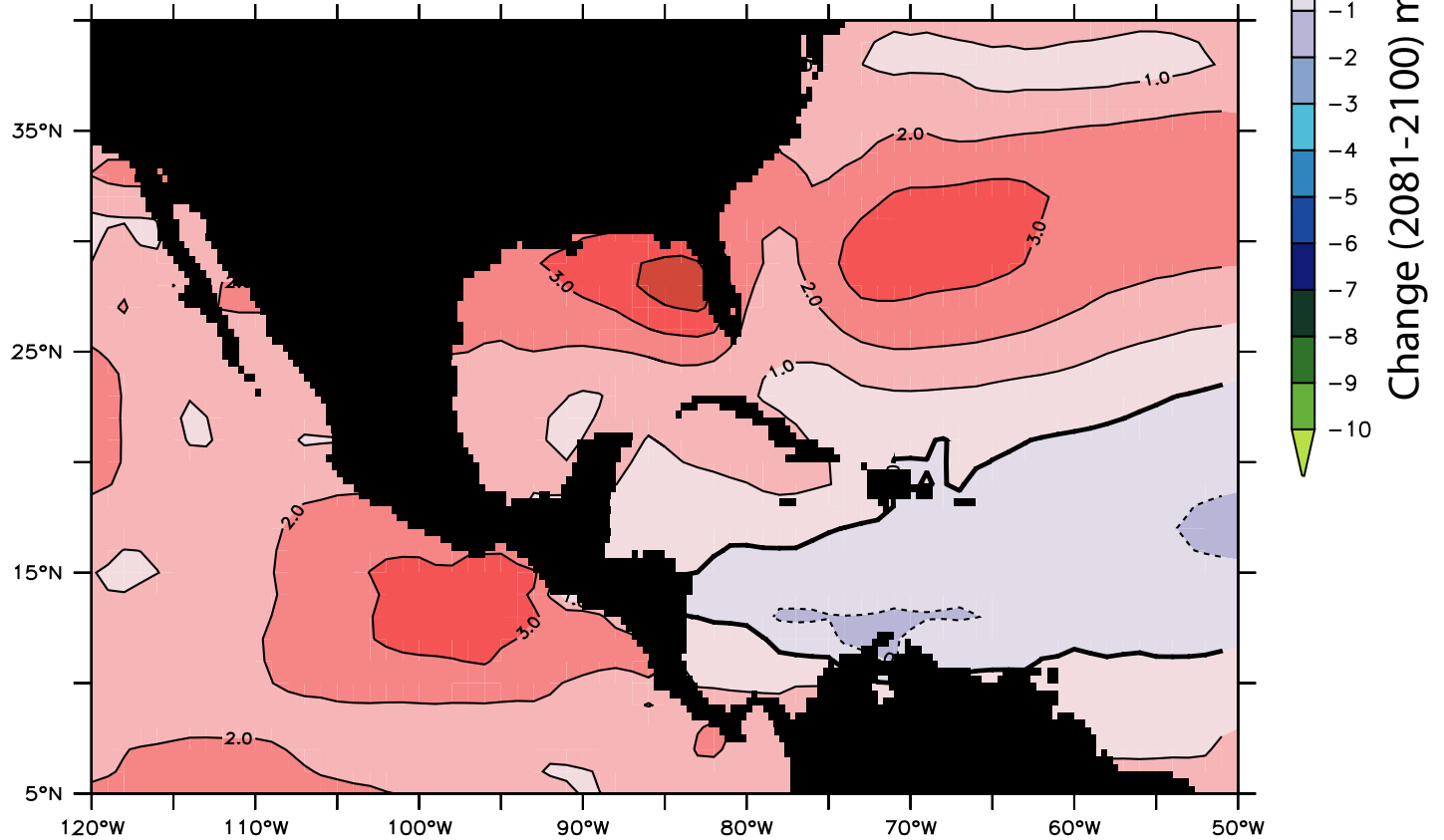
Supplementary Figure 2: Estimates of the impact of (a) shear and (b) large-scale thermodynamic conditions on North Atlantic and East Pacific tropical storms, based on the IPCC AR-4 Scenario A1B multi-model ensemble-mean change. (a) Impact of model project changes in shear to the intensity computed by applying the *DeMaria [1996]* latitude-dependent regression between shear and storm intensity change to the tropical storms in the 1965-2006 U.S. National Hurricane Center Best Track Database – sampling the model-projected June-November (850hPa-200hPa) shear change along the storm tracks. Symbols are plotted such that symbols of larger amplitude overlay those of lower amplitude, and when symbols have the same amplitude those of positive sign overlay those of negative sign. (b) Change in the June-November *Emanuel [1995]* maximum potential intensity of tropical storm velocity (MPI_v), for the IPCC-AR4 Scenario A1B multi-model ensemble-mean. Changes computed as differences between the period (2081-2100) and (2001-2020); units for the changes in ms^{-1}. Notice that the magnitude of the changes to intensity at storm landfall from changes in shear are comparable to those of MPI_v, and generally acting to reduce storm intensity.

December through May IPCC-AR4 Scenario A1B Projected 21st Century Changes
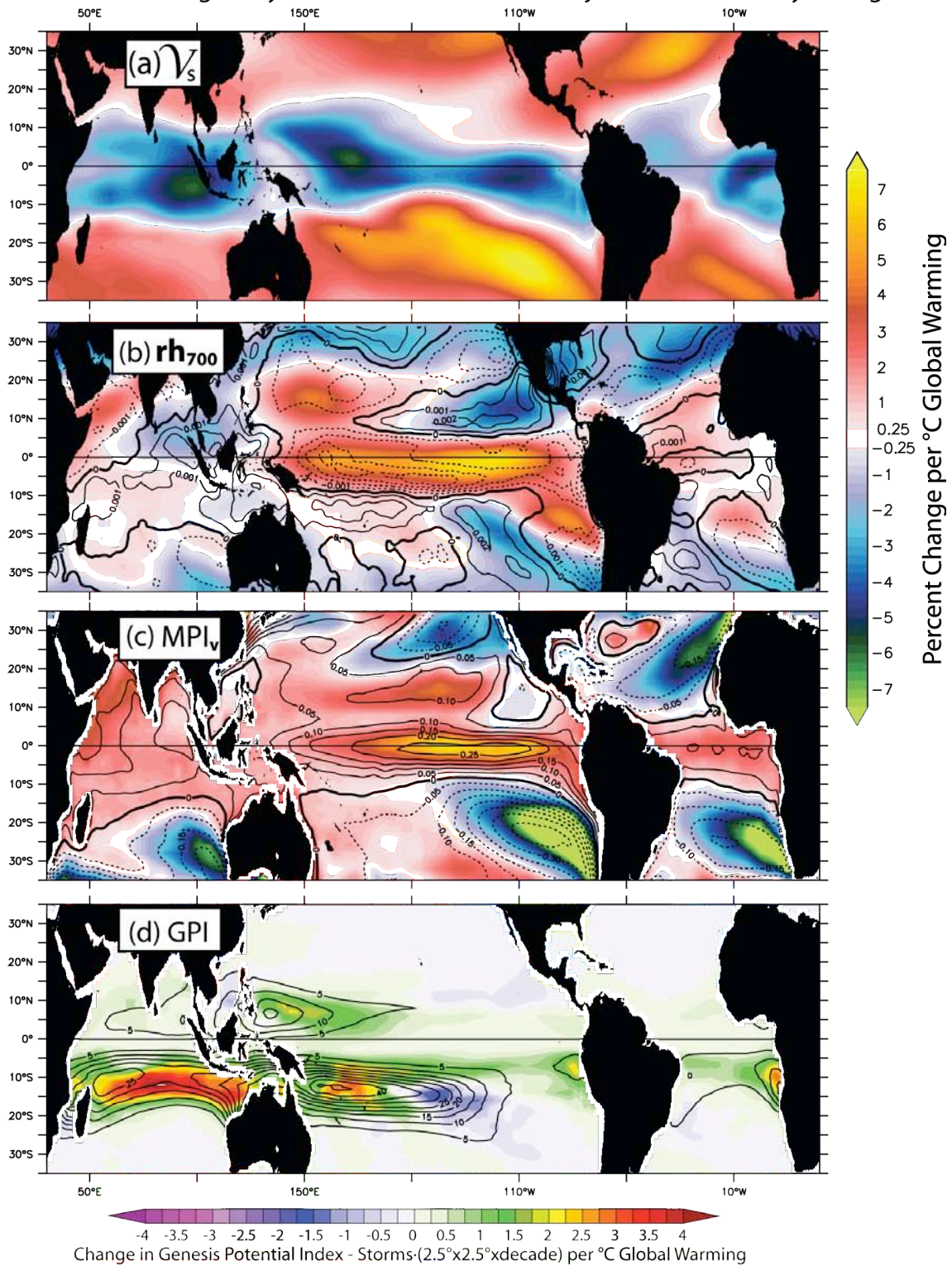
Supplementary Figure 3: Same as Figure 4 except for the six month season December-May: IPCC-AR4 Scenario A1B ensemble mean projected fractional change in large-scale environmental parameters associated with hurricane intensity and activity: (a) V_s, (b) 700hPa relative humidity, and (c) *Emanuel [1995]* wind maximum potential intensity (MPI_v). Panel (d) shows the change in *Emanuel and Nolan [2004]* genesis potential index (GPI). Fractional changes are normalized by global surface air temperature increase. Contoured in (b) is the ensemble-mean 500hPa pressure velocity (ω_{500}) change (normalized by each model's global mean surface temperature change), upward motion is negative. Contoured in (c) is the difference between the local SST change and the 35°S-35°N mean SST change, normalized by the 35°S-35°N mean SST change. Contoured in (d) is the ensemble-mean GPI averaged over the period 2001-2020.